Directional Localization from a Magnetic Field in Moiré Systems

Nisarga Paul[*], Philip J. D. Crowley,[*] and Liang Fu

Department of Physics, Massachusetts Institute of Technology, Cambridge, Massachusetts, USA

Moiré materials provide a highly tunable platform in which novel electronic phenomena can emerge. We study strained moiré materials in a uniform magnetic field and predict highly anisotropic electrical conductivity that switches easy axis as magnetic field or strain is varied. The dramatic anisotropy reflects one-dimensional localization (directional localization) of the electron wave functions along a crystal axis due to quantum interference effects. This can be understood in an effective one-dimensional quasiperiodic Aubry-André-Harper-like model, or in a complementary semiclassical picture. This phenomenon should be observable in strained moiré materials at realistic fields and low strain disorder, as well as unstrained systems with anisotropic Fermi surfaces.

Introduction.—The advent of moiré materials has recently unlocked new opportunities for the control and engineering of two-dimensional quantum phases of matter [1–9]. When subject to a quantizing magnetic field, moiré systems exhibit a complex energy spectrum due to the interplay between Landau level physics and the moiré superlattice [10–15]. Indeed, unlike ordinary semiconductors, a key feature of moiré systems is that the magnetic length ℓ and moiré lattice constant a_M are often comparable, both on the order of tens of nanometers. This allows access to two distinct sets of phenomena. First, the electronic spectrum exhibits fractal Hofstadter features, including Brown-Zak oscillations [16–18], due to the moiré unit cell enclosing $O(1)$ flux quanta [19], as observed in graphene-hexagonal boron nitride [10–12]. Second, the destructive interference between the Landau level orbitals and the moiré potential result in band flattenings, or magic zeros, at a discrete set of magnetic fields, and other commensurability phenomena [20,21].

Strain is ubiquitous in realistic moiré materials. Since a small strain at the atomic scale is magnified by the large superlattice period, strain often plays an important role in understanding the phenomenology of the system [22–26]. Recent experimental advances in 2D materials also promise greater control over strain as a tuning knob, paving the way for "strain engineering" [27] or "straintronics" [28]. The effect of strain on magnetotransport has just started to be studied experimentally and theoretically [29,30].

In this Letter, we show that strain provides an avenue to new physics in moiré superlattices: namely, the combination of strain (specifically, uniaxial or shear heterostrain) and magnetic field generally induces one-dimensional electronic states, leading to highly anisotropic magnetotransport (Fig. 1). Moreover, the resistivity anisotropy, including the transport easy axis, is strongly tunable by carrier density ρ or field. At fixed ρ, it alternates periodically in $1/B$ with period $\sim 2k_F/a_M$. This is due to an effective dimensional reduction of the 2D system to an array of 1D extended states. We support this picture in two complementary limits: in the high field limit, the origin of this directional localization is the noncommutativity of projected position operators x and y in the effective picture of the Landau level perturbed by the moiré potential, while in the low field limit, a semiclassical scattering model reproduces the same results. We emphasize that this is a quantum interference phenomenon largely independent of the microscopic details of the moiré system. While highly anisotropic transport has been observed in moiré materials with a 1D superlattice structure [31–33], in our case the transport anisotropy varies periodically in $1/B$. Because of its universality and robustness, we expect field-induced directional localization is a readily observable effect in moiré systems that is beyond the purview of traditional solids.

Directional localization from strain and field.—First, let us review our expectations for magnetotransport in the 2D electron systems. In a clean system, when the Fermi level is between Landau levels, we expect familiar quantum Hall plateaus with vanishing σ_{ii} ($i = x, y$) and σ_{xy} quantized to $e^2\nu/h$. As the Fermi level sweeps through a Landau level, plateau transitions occur in σ_{xy} and σ_{ii} exhibits a peak.
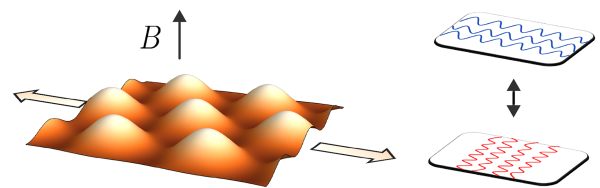

FIG. 1. 1D localization in strained moiré systems. We consider strained moiré systems in a perpendicular field. The result is highly anisotropic conductivity that switches direction with ρ. This phenomenon is universal, accessible, and robust to strain disorder.

Our focus is on these peaks, and in particular oscillations of their heights. Specifically, we predict drastic anisotropy in the longitudinal conductivities in moiré systems due to the (generic) presence of strain.

To proceed, our starting point is the continuum Hamiltonian ($\hbar = 1$)

$$H = H_0(\boldsymbol{p} - e\boldsymbol{A}) + V(\boldsymbol{r}), \qquad (1)$$

which describes electrons minimally coupled to a uniform magnetic field in the presence of a moiré potential. We consider a moiré potential,

$$V(\boldsymbol{r}) = \sum_i V_i e^{i\boldsymbol{Q}_i \cdot \boldsymbol{r}}, \qquad (2)$$

built out of long-wavelength harmonics with $Q_i \sim 1/a_M$. Let us specialize for now to a quadratic dispersion $H_0(\boldsymbol{p}) = p^2/2m$. When $V = 0$, the spectrum is described by Landau levels with energy $E_n = \omega_c(n + 1/2)$, where $\omega_c = eB/m$. For small V_0/ω_c, the Landau levels acquire a bandwidth of order V_0 and we can work within a low-energy effective theory. The effective Hamiltonian in the nth Landau level is given by $\tilde{V} = P_n V P_n$, where P_n is the corresponding projector. Adopting a symmetric gauge, we find

$$\tilde{V}(\tilde{\boldsymbol{r}}) = \sum_i \tilde{V}_i e^{i\boldsymbol{Q}_i \cdot \tilde{\boldsymbol{r}}} \qquad (3)$$

to leading order, where $\tilde{V}_i = V_i e^{-Q_i^2 \ell^2/4} L_n(Q_i^2 \ell^2/2)$ and L_n is the nth Laguerre polynomial. Here, $\tilde{\boldsymbol{r}} = (\tilde{x}, \tilde{y})$ are the projected position operators, which satisfy

$$[\tilde{x}, \tilde{y}] = i\ell^2. \qquad (4)$$

Consider first the example of a *square* superlattice potential, $V(\boldsymbol{r}) = 2V_0[\cos Q_x x + \cos Q_y y]$. The projected potential is

$$\tilde{V}(\tilde{\boldsymbol{r}}) = 2\tilde{V}_x \cos Q_x \tilde{x} + 2\tilde{V}_y \cos Q_y \tilde{y}. \qquad (5)$$

Let $\beta = 2\pi/Q_x Q_y \ell^2$ be the magnetic flux per unit cell in units of $\hbar/e$. Then we may write

$$\tilde{V} = 2\tilde{V}_y(\cos Y + \lambda \cos X), \quad [X, Y] = 2\pi i/\beta, \qquad (6)$$

where $\lambda = \tilde{V}_x/\tilde{V}_y$. Let $X|x\rangle = x|x\rangle$ and let $c_j^\dagger$ create the state $|\phi_j/Q_x\rangle$ where $\phi_j = \phi_0 + 2\pi j/\beta$. For each ϕ_0, we may regard $\tilde{V}$ as a 1D tight-binding model,

$$\tilde{V} = \sum_j 2\tilde{V}_x \cos(\phi_j) c_j^\dagger c_j + \tilde{V}_y (c_{j+1}^\dagger c_j + \text{H.c.}). \qquad (7)$$

This is equivalent to the Aubry-André-Harper (AAH) model [34], a canonical model that exhibits a localization-delocalization transition at $|\lambda| = 1$. This is consistent with the duality of Eq. (6) under $X \leftrightarrow Y$ and $\lambda \leftrightarrow 1/\lambda$. In the presence of strict C_4 rotational symmetry, $\lambda = 1$ and the model is at its critical point. However, any superlattice strain [35] results in $Q_x \neq Q_y$ and can have stark effects, as λ, being the ratio of oscillating functions, fluctuates dramatically about the critical point. The appearance of the AAH model in the study of Bloch electrons in a magnetic field has been noted [44].

Previous studies have shown that this transition is sharp if and only if β is a "Diophantine number" [36], which is a dense subset of the irrationals that excludes Liouville numbers (for which the wave functions never localize [45]). The existence of localized and delocalized phases at generic β, possibly separated by a mobility edge near $\lambda = 1$, has been verified numerically [46].

Consider next the more realistic case of a *triangular* superlattice cosine potential, $V(\boldsymbol{r}) = \sum_{i=1}^3 2V_i \cos \boldsymbol{Q}_i \cdot \boldsymbol{r}$, with $\boldsymbol{Q}_i = Q\{\cos[2\pi(i-1)/3], \sin[2\pi(i-1)/3]\}$. The projected potential can be written [47]

$$\tilde{V} = \sum_{i=1}^3 2\tilde{V}_i \cos X_i, \qquad [X_j, X_{j+1}] = 2\pi i/\beta, \qquad (8)$$

where $X_i = \boldsymbol{Q}_i \cdot \tilde{\boldsymbol{r}}$ and $\beta = 2\pi/|\boldsymbol{Q}_1 \times \boldsymbol{Q}_2|\ell^2$. For $\tilde{V}_2 = \tilde{V}_3$, consider an X_1 eigenbasis $|x_1\rangle$ and let $c_j^\dagger$ create $|\phi_j/Q_1\rangle$, where $\phi_j = \phi_0 + 2\pi j/\beta$. Then for each ϕ_0, we may again regard $\tilde{V}$ as a 1D tight-binding model,

$$\tilde{V} = \sum_j 2\tilde{V}_1 \cos(\phi_j) c_j^\dagger c_j$$
$$+ 2\tilde{V}_2 \cos(\phi_{j+1/2}/2)(c_{j+1}^\dagger c_j + \text{H.c.}). \qquad (9)$$

In both of the examples Eqs. (6) and (8), the presence of strain results in rapid switching between localized and delocalized regimes in the effective models with varying magnetic field. This implies a 1D localization in the 2D model along a direction that switches with varying magnetic field. For instance, in the square lattice case, for $|\tilde{V}_y| > |\tilde{V}_x|$ we expect wave functions localized along the y direction, and for $|\tilde{V}_x| > |\tilde{V}_y|$, we expect wave functions localized along x.

So far, we have discussed the square and triangular lattice cosine potentials in the perturbative regime. In fact, this perturbative result holds for any 2D periodic potential $V(\boldsymbol{r})$. In the absence of strain, $V(\boldsymbol{r})$ and $\tilde{V}(\tilde{\boldsymbol{r}})$ possess rotational symmetry. In the presence of strain, the eigenmodes of $\tilde{V}(\tilde{\boldsymbol{r}})$ are generically delocalized in one direction and localized in the perpendicular direction. The localization direction may be simply read off from the functional form of $\tilde{V}(\tilde{\boldsymbol{r}})$: it is the direction in which $\tilde{V}(\tilde{\boldsymbol{r}})$ has extended level sets (i.e., open orbits). This direction is uniquely defined for generic $\tilde{V}(\tilde{\boldsymbol{r}})$, as the extended level sets of a 2D

periodic function necessarily all run parallel to the same lattice vector $\boldsymbol{b}_{ext}$. As $\tilde{V}(\tilde{\boldsymbol{r}})$ is varied by tuning the strain, the direction of the extended level sets $\boldsymbol{b}_{ext}$ can discretely switch along crystal directions [48–51,52]. At the critical points where $\boldsymbol{b}_{ext}$. changes (including in the zero-strain case), the wave functions are critically delocalized in all directions.

While the discussion has so far dealt with the perturbative regime, we now demonstrate that this phenomenon is nonperturbative, and moreover holds for quite general energy dispersions. Our starting point is the semiclassical equations of motion for a Bloch wave packet,

$$\dot{\boldsymbol{p}} = -e\dot{\boldsymbol{r}} \times \boldsymbol{B}, \qquad \dot{\boldsymbol{r}} = \boldsymbol{\nabla} E(\boldsymbol{p}), \tag{10}$$

where $E(\boldsymbol{p})$ is the energy dispersion including the effect of the moiré potential.

The relevant degrees of freedom at low temperatures are the electronic states near the Fermi surface. Wave packets formed of these states can be thought of as propagating in a network made of copies of the *original* Fermi surface separated by the superlattice wave vectors $\boldsymbol{Q}_j$. We will consider the case of a strained square moiré superlattice, $Q_x \neq Q_y$. Away from the junctions, electrons propagate freely and unidirectionally according to Eq. (10) while picking up Aharanov-Bohm phases. Near the junctions, two incoming modes scatter into two outgoing modes, which is properly described as a Landau-Zener two-level crossing with scattering unitary

$$U = \begin{pmatrix} \sqrt{1-P}e^{-i\bar{\varphi}_S} & -\sqrt{P} \\ \sqrt{P} & \sqrt{1-P}e^{i\bar{\varphi}_S} \end{pmatrix}, \tag{11}$$

where the P is the magnetic breakdown probability,

$$P = e^{-2\pi/\delta}, \qquad \delta = 16eBv_1v_2 \sin\beta/E_{gap}^2. \tag{12}$$

Here, $\boldsymbol{v}_1$ and $\boldsymbol{v}_2$ are the velocities of incoming electrons, $\hat{\boldsymbol{v}}_1 \cdot \hat{\boldsymbol{v}}_2 = \cos\beta$, $E_{gap} = 2V_0$ is the band gap at the Bragg plane due to moiré potential, and $\tilde{\varphi}_S = \varphi_S - \pi/2$ with $\varphi_S = \pi/4 - (\ln\delta + 1)/\delta + \arg\Gamma(1 - i/\delta)$ [20,53]. The form of P makes clear that this approach is nonperturbative in V_0/ω_c. We refer to [54–57] for other examples of semiclassical network constructions. We remark that the regime of validity of the semiclassical approximation in this setting is large Landau level index.

Because of the periodicity of the repeated Brillouin zone, energy eigenstates are Bloch-periodic eigenmodes of the network model. For this, it is instructive to study the scattering matrices W_x and W_y across the intersections of Fermi surfaces, which we call the "lens orbits," as indicated in Fig. 2. These take the form [20]
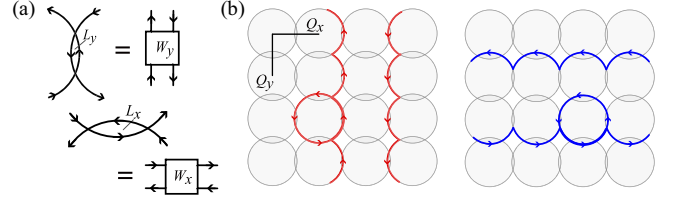

FIG. 2. Semiclassical approach. (a) W_i denotes the scattering unitary across the lens orbit L_i ($i = x, y$). (b) Fermi surfaces in the repeated zone scheme with moiré wave vectors $Q_x > Q_y$, with example semiclassical trajectories when electron motion is entirely in the ith direction, which occurs at the quantization condition Eq. (14).

$$W_i = \frac{1}{(1-P_i)e^{i(\xi_i+2\bar{\varphi}_{S,i})} - 1} \begin{pmatrix} P_i e^{i\xi_i/2} & \kappa_i \\ \kappa_i & P_i e^{i\xi_i/2} \end{pmatrix} \tag{13a}$$

$$\kappa_i = e^{-i\bar{\varphi}_{S,i}}\sqrt{1-P_i}(e^{i(\xi_i+2\bar{\varphi}_{S,i})} - 1), \tag{13b}$$

where $\xi_i = \ell^2 S(L_i)$ and $S(L_i)$ is the k-space area of L_i. When $\kappa_i = 0$, W_i is purely diagonal, implying that electron motion is entirely in the ith direction ($i = x, y$). In other words, the junctions of L_i are "transparent" to the electrons. The condition for electron motion to be entirely in the i direction is thus $\kappa_i = 0$ or

$$\ell^2 S(L_i) + 2\tilde{\varphi}_{S,i} = 2\pi n, \tag{14}$$

where $n \in \mathbb{Z}$. This is a Bohr-Sommerfeld quantization condition for L_i.

If $S(L_x) = S(L_y)$, then Eq. (14) is satisfied simultaneously for x and y if at all, and electron motion always remains delocalized in both directions. In the presence of any strain, however, $S(L_x) \neq S(L_y)$, so that electron motion can alternate between strict localization in x and y, corroborating the perturbative approach. This approach places only topological constraints on the shape of the Fermi surface, and reveals that this phenomenon generalizes broadly and does not rely on perturbation theory, though agreement with the perturbative method obtains for large n [20].

Magnetotransport.—To reveal the observable effects, we turn to a study of magnetotransport in strained moiré superlattices. Conductivity can be taken as $\sigma_{ab} = D_{ab}\tau$ under the assumption of a single relaxation time τ, where D_{ab} is the Drude weight [37],

$$D_{ab} = -ie\langle[j_a, x_b]\rangle_0 + A\sum_{n\neq m}f_{nm}\frac{[j_a]_{nm}[j_b]_{mn}}{E_n - E_m}. \tag{15}$$

Here, j_a is the current density operator, $f_{nm} = f_n - f_m$, where $f_n = (1 + e^{\beta(E_n-\mu)})^{-1}$ is the Fermi-Dirac distribution, and A is the sample area. We derive this for completeness in the Supplemental Material [35]. As an example, for a Fermi

gas, $\boldsymbol{j} = -e\boldsymbol{p}/mA$ and $\sigma_{ab} = (ie^2\tau/mA)\langle[p_a, x_b]\rangle_0 = (ne^2\tau/m)\delta_{ab}$ is the familiar Drude conductivity.

For a general Hamiltonian $H = T + V$ with $T = \sum_n E_n P_n$ (for projectors P_n) and V small, for any operator M we may consider the projected low-energy operator $\tilde{M}$ that satisfies $\langle\psi_1|M|\psi_2\rangle = \langle\tilde{\psi}_1|\tilde{M}|\tilde{\psi}_2\rangle$ for all energy eigenstates $|\psi_i\rangle$, and with $|\tilde{\psi}_i\rangle = P_n|\psi_i\rangle$. Expanding perturbatively in V, this is given by

$$\tilde{M} = P_n M P_n + \sum_{m \neq n} \frac{P_n M P_m V P_n - P_n V P_m M P_n}{E_n - E_m} + O(V^2). \tag{16}$$

The low-energy effective current density operator is given to leading order by

$$\tilde{\boldsymbol{j}} = ie[\tilde{\boldsymbol{r}}, \tilde{V}]/A \tag{17a}$$

$$= e\ell^2 \sum_i (\hat{z} \times \boldsymbol{Q}_i)\tilde{V}_i e^{i\boldsymbol{Q}_i \cdot \tilde{\boldsymbol{r}}}/A \tag{17b}$$

by application of Eq. (16). Note that $\tilde{\boldsymbol{j}}$ vanishes to zeroth order in V, as the bare current operator $\boldsymbol{j}$ only couples neighboring Landau levels. Finally, conductivity may be computed to leading order in V/ω_c using the effective operators $\tilde{V}, \tilde{\boldsymbol{r}}, \tilde{\boldsymbol{j}}$ in Eq. (15).

In Fig. 3, we use this method to plot longitudinal conductivities in the presence of a magnetic field and strain for square and triangular superlattices. Evidently σ_{xx} and σ_{yy} show dramatic oscillations, consistent with our picture of localization-delocalization transitions, for the square superlattice, while σ_{xx} does so for the triangular superlattice with milder oscillations in σ_{yy}. We note that the x, y asymmetry in the triangular lattice case originates from
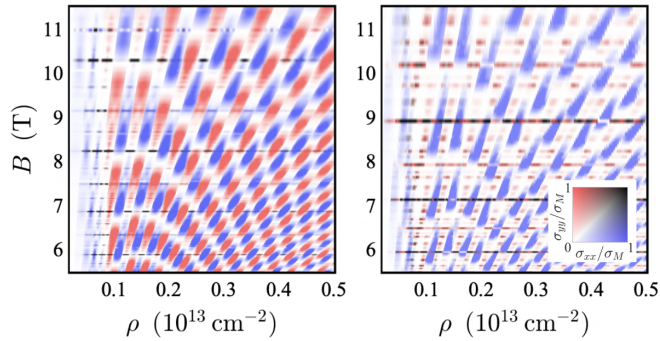

FIG. 3. Conductivity switching. σ_{xx} and σ_{yy} in a strained square (left) and triangular (right) lattice and magnetic field, with uniaxial strain $x \mapsto \alpha x$, $y \mapsto \alpha^{-1}y$, $\alpha = 0.98$. The ratio σ_{xx}/σ_{yy} is plotted in color, with the intensity proportional to average magnitude up to maximum σ_M. We observe sharp conductivity anisotropy that switches as a function of B/density. Horizontal dark features are Brown-Zak oscillations at flux $1/q$ per unit cell. ($Q = 2\pi/10$ nm^{-1}, $V_0 = 5$ meV, $T = 0.5$ meV).

the principal strain axes aligning with only $\boldsymbol{Q}_1 \| \hat{x}$. We also note the presence of Brown-Zak oscillations (horizontal features) at small-numerator rational flux values.

We can infer the frequency of the directional switching as follows. In the presence of two unequal wave vectors $Q_1 \neq Q_2$, the switching is driven by the parameter $\lambda = \tilde{V}_1/\tilde{V}_2$, which at large Landau level index n behaves as

$$\lambda \approx \sqrt{\frac{Q_2}{Q_1}} \frac{\cos(\sqrt{2n}Q_1\ell - \pi/4)}{\cos(\sqrt{2n}Q_2\ell - \pi/4)}, \tag{18}$$

where we used a large n approximation to Laguerre polynomials [58]. The ratio of two incommensurate harmonics ω, ω' generically exhibits fast and slow oscillations at frequencies $\omega + \omega'$ and $|\omega - \omega'|$. Relating density to Landau level index by $n = 2\pi\rho\ell^2$, we conclude that the fast oscillations are periodic in $1/B$ with frequency

$$\omega_0 = \sqrt{4\pi\rho}(Q_1 + Q_2) \tag{19}$$

and slow modulating features are present at frequency $\sqrt{4\pi\rho}|Q_1 - Q_2|$ (visible for larger strain).

When $Q_1 \sim Q_2$, $\omega_0 \sim 2k_F Q$, which is the familiar frequency of Weiss oscillations in $1/B$ [20]. However, while Weiss oscillations exist even in a 1D potential, the phenomenon at hand requires a 2D potential, and thus it consolidates both Hofstadter and commensurability physics.

Discussion.—We have discussed a series of transitions between highly anisotropic conductivities in the same universality class as the localization-delocalization transition of the AAH model, which can be readily observed in magnetotransport experiments on strained moiré materials. This is a manifestation of "directional localization" due to the fundamental quantum noncommutativity of position operators in the presence of a magnetic field.

In fact, this phenomenon can be observed more broadly in 2D materials with anisotropic Fermi surfaces and in a nonperturbative regime $V_0 \gtrsim \omega_c$, as we have demonstrated using a semiclassical approach. However, the magnetic length should be on the order of the lattice constant, making this difficult to realize outside moiré materials.

Our predictions are remarkably robust to strain disorder, which is omnipresent in moiré systems [35]. At large fields ($B \gtrsim \sqrt{\rho}Q$), no reasonable strain disorder disrupts homogeneous 1D localization. At small fields ($B \ll \sqrt{\rho}Q$) a strain disorder up to $\delta\alpha \sim \sqrt{B/\sqrt{\rho}Q}$ is tolerable. For instance at $B = 5$ T, $Q = 2\pi/10$ nm^{-1} and one electron per unit cell, up to 30% is permissible (far larger than the strain disorder in many clean moiré graphene samples). This is consistent with the fact that the switching frequency ω_0 depends quite weakly on strain. A more detailed discussion of strain disorder is given in the Supplemental Material [35].

We remark that evidence for unusual magnetotransport in moiré systems has been previously found in related

contexts. Reference [59] observed unusual magnetotransport in twisted bilayer graphene that was captured well by an anisotropic Hofstadter model. Such a model was also studied in Ref. [60], which noted enhanced σ_{xx}/σ_{yy}, but no "switching".

One intriguing question for future work is whether this effect can be achieved in a general Chern band or in the absence of magnetic field. Indeed, the fundamental noncommutativity of the projected position operators depends only on the quantum geometry of the band. Other interesting directions for future studies include possible technological applications of this phenomenon, such as for "moiré transistors" or magnetic sensors.

---

[*] These authors contributed equally to this letter.

[1] Y. Cao, V. Fatemi, S. Fang, K. Watanabe, T. Taniguchi, E. Kaxiras, and P. Jarillo-Herrero, Unconventional superconductivity in magic-angle graphene superlattices, Nature (London) **556**, 43 (2018).

[2] E. Y. Andrei and A. H. MacDonald, Graphene bilayers with a twist, Nat. Mater. **19**, 1265 (2020).

[3] K. F. Mak and J. Shan, Semiconductor moiré materials, Nat. Nanotechnol. **17**, 686 (2022).

[4] E. Y. Andrei, D. K. Efetov, P. Jarillo-Herrero, A. H. MacDonald, K. F. Mak, T. Senthil, E. Tutuc, A. Yazdani, and A. F. Young, The marvels of moire materials, Nat. Rev. Mater. **6**, 201 (2021).

[5] Y. Cao, V. Fatemi, A. Demir, S. Fang, S. L. Tomarken, J. Y. Luo, J. D. Sanchez-Yamagishi, K. Watanabe, T. Taniguchi, E. Kaxiras, R. C. Ashoori, and P. Jarillo-Herrero, Correlated insulator behaviour at half-filling in magic-angle graphene superlattices, Nature (London) **556**, 80 (2018).

[6] Y. Cao, D. Rodan-Legrain, O. Rubies-Bigorda, J. M. Park, K. Watanabe, T. Taniguchi, and P. Jarillo-Herrero, Tunable correlated states and spin-polarized phases in twisted bilayer–bilayer graphene, Nature (London) **583**, 215 (2020).

[7] J. M. Park, Y. Cao, K. Watanabe, T. Taniguchi, and P. Jarillo-Herrero, Tunable strongly coupled superconductivity in magic-angle twisted trilayer graphene, Nature (London) **590**, 249 (2021).

[8] Y. Tang, L. Li, T. Li, Y. Xu, S. Liu, K. Barmak, K. Watanabe, T. Taniguchi, A. H. MacDonald, J. Shan, and K. F. Mak, Simulation of Hubbard model physics in WSe_2/WS_2 moiré superlattices, Nature (London) **579**, 353 (2020).

[9] T. Li, S. Jiang, B. Shen, Y. Zhang, L. Li, Z. Tao, T. Devakul, K. Watanabe, T. Taniguchi, L. Fu, J. Shan, and K. F. Mak, Quantum anomalous Hall effect from intertwined moiré bands, Nature (London) **600**, 641 (2021).

[10] C. R. Dean, L. Wang, P. Maher, C. Forsythe, F. Ghahari, Y. Gao, J. Katoch, M. Ishigami, P. Moon, M. Koshino, T. Taniguchi, K. Watanabe, K. L. Shepard, J. Hone, and P. Kim, Hofstadter's butterfly and the fractal quantum Hall effect in moiré superlattices, Nature (London) **497**, 598 (2013).

[11] L. A. Ponomarenko, R. V. Gorbachev, G. L. Yu, D. C. Elias, R. Jalil, A. A. Patel, A. Mishchenko, A. S. Mayorov, C. R. Woods, J. R. Wallbank, M. Mucha-Kruczynski, B. A. Piot, M. Potemski, I. V. Grigorieva, K. S. Novoselov, F. Guinea, V. I. Fal'ko, and A. K. Geim, Cloning of Dirac fermions in graphene superlattices, Nature (London) **497**, 594 (2013).

[12] B. Hunt, J. D. Sanchez-Yamagishi, A. F. Young, M. Yankowitz, B. J. LeRoy, K. Watanabe, T. Taniguchi, P. Moon, M. Koshino, P. Jarillo-Herrero, and R. C. Ashoori, Massive Dirac fermions and hofstadter butterfly in a van der Waals heterostructure, Science **340**, 1427 (2013).

[13] E. M. Spanton, A. A. Zibrov, H. Zhou, T. Taniguchi, K. Watanabe, M. P. Zaletel, and A. F. Young, Observation of fractional Chern insulators in a van der Waals heterostructure, Science **360**, 62 (2018).

[14] Y. Xie, A. T. Pierce, J. M. Park, D. E. Parker, E. Khalaf, P. Ledwith, Y. Cao, S. H. Lee, S. Chen, P. R. Forrester, K. Watanabe, T. Taniguchi, A. Vishwanath, P. Jarillo-Herrero, and A. Yacoby, Fractional Chern insulators in magic-angle twisted bilayer graphene, Nature (London) **600**, 439 (2021).

[15] C. R. Kometter, J. Yu, T. Devakul, A. P. Reddy, Y. Zhang, B. A. Foutty, K. Watanabe, T. Taniguchi, L. Fu, and B. E. Feldman, Hofstadter states and reentrant charge order in a semiconductor moiré lattice, arXiv:2212.05068.

[16] R. Krishna Kumar, A. Mishchenko, X. Chen, S. Pezzini, G. H. Auton, L. A. Ponomarenko, U. Zeitler, L. Eaves, V. I. Fal'ko, and A. K. Geim, High-order fractal states in graphene superlattices, Proc. Natl. Acad. Sci. U.S.A. **115**, 5135 (2018).

[17] Y. Yang, J. Li, J. Yin, S. Xu, C. Mullan, T. Taniguchi, K. Watanabe, A. K. Geim, K. S. Novoselov, and A. Mishchenko, In situ manipulation of van der Waals heterostructures for twistronics, Sci. Adv. **6**, eabd3655 (2020).

[18] R. Huber, M.-N. Steffen, M. Drienovsky, A. Sandner, K. Watanabe, T. Taniguchi, D. Pfannkuche, D. Weiss, and J. Eroms, Band conductivity oscillations in a gate-tunable graphene superlattice, Nat. Commun. **13**, 1 (2022).

[19] D. R. Hofstadter, Energy levels and wave functions of Bloch electrons in rational and irrational magnetic fields, Phys. Rev. B **14**, 2239 (1976).

[20] N. Paul, P. J. D. Crowley, T. Devakul, and L. Fu, Moiré Landau fans and magic zeros, Phys. Rev. Lett. **129**, 116804 (2022).

[21] D. Weiss, K. V. Klitzing, K. Ploog, and G. Weimann, Magnetoresistance oscillations in a two-dimensional electron gas induced by a submicrometer periodic potential, Europhys. Lett. **8**, 179 (1989).

[22] Z. Bi, N. F. Q. Yuan, and L. Fu, Designing flat bands by strain, Phys. Rev. B **100**, 035448 (2019).

[23] F. Mesple, A. Missaoui, T. Cea, L. Huder, F. Guinea, G. Trambly de Laissardière, C. Chapelier, and V. T. Renard, Heterostrain determines flat bands in magic-angle twisted graphene layers, Phys. Rev. Lett. **127**, 126405 (2021).

[24] G. Shavit, K. Kolar, C. Mora, F. von Oppen, and Y. Oreg, Strain disorder and gapless intervalley coherent phase in twisted bilayer graphene, Phys. Rev. B **107**, L081403 (2023).

[25] H. Zheng, D. Zhai, and W. Yao, Twist versus heterostrain control of optical properties of moiré exciton minibands, 2D Mater. **8,** 044016 (2021).

[26] K. P. Nuckolls, R. L. Lee, M. Oh, D. Wong, T. Soejima, J. P. Hong, D. Calugaru, J. Herzog-Arbeitman, B. A. Bernevig, K. Watanabe, T. Taniguchi, N. Regnault, M. P. Zaletel, and A. Yazdani, Quantum textures of the many-body wavefunctions in magic-angle graphene, Nature (London) **620,** 525 (2023).

[27] Z. Peng, X. Chen, Y. Fan, D. J. Srolovitz, and D. Lei, Strain engineering of 2D semiconductors and graphene: From strain fields to band-structure tuning and photonic applications, Light Sci. Appl. **9,** 1 (2020).

[28] F. Miao, S.-J. Liang, and B. Cheng, Straintronics with van der Waals materials, npj Quantum Mater. **6,** 1 (2021).

[29] O. Vafek, Anisotropic resistivity tensor from disk geometry magneto-transport, Phys. Rev. Appl. **20,** 064008 (2023).

[30] X. Wang, J. Finney, A. L. Sharpe, L. K. Rodenbach, C. L. Hsueh, K. Watanabe, T. Taniguchi, M. A. Kastner, O. Vafek, and D. Goldhaber-Gordon, Unusual magnetotransport in twisted bilayer graphene from strain-induced open Fermi surfaces, Proc. Natl. Acad. Sci. U.S.A. **120,** e2307151120 (2023).

[31] P. Wang, G. Yu, Y. H. Kwan, Y. Jia, S. Lei, S. Klemenz, F. A. Cevallos, R. Singha, T. Devakul, K. Watanabe, T. Taniguchi, S. L. Sondhi, R. J. Cava, L. M. Schoop, S. A. Parameswaran, and S. Wu, One-dimensional Luttinger liquids in a two-dimensional moiré lattice, Nature (London) **605,** 57 (2022).

[32] D. M. Kennes, L. Xian, M. Claassen, and A. Rubio, One-dimensional flat bands in twisted bilayer germanium selenide, Nat. Commun. **11,** 1 (2020).

[33] D. Beret, I. Paradisanos, H. Lamsaadi, Z. Gan, E. Najafidehaghani, A. George, T. Lehnert, J. Biskupek, U. Kaiser, S. Shree, A. Estrada-Real, D. Lagarde, X. Marie, P. Renucci, K. Watanabe, T. Taniguchi, S. Weber, V. Paillard, L. Lombez, J.-M. Poumirol, A. Turchanin, and B. Urbaszek, Exciton spectroscopy and unidirectional transport in MoSe$_2$-WSe$_2$ lateral heterostructures encapsulated in hexagonal boron nitride, npj 2D Mater. Appl. **6,** 1 (2022).

[34] S. Aubry and G. André, Analyticity breaking and Anderson localization in incommensurate lattices, Ann. Isr. Phys. Soc. **3,** 133 (1980).

[35] See Supplemental Material at http://link.aps.org/supplemental/10.1103/PhysRevLett.132.246402 which includes Refs. [36–43], for general discussion of strain in moiré bilayers, shear strain, details on the effective AAH models and transport calculation, and the role of strain disorder.

[36] S. Ya. Jitomirskaya, Metal-insulator transition for the almost Mathieu operator, Ann. Math. **150,** 1159 (1999).

[37] R. Resta, Drude weight and superconducting weight, J. Phys. Condens. Matter **30,** 414001 (2018).

[38] D. J. Scalapino, S. R. White, and S. Zhang, Insulator, metal, or superconductor: The criteria, Phys. Rev. B **47,** 7995 (1993).

[39] W. Kohn, Cyclotron resonance and de Haas-van Alphen oscillations of an interacting electron gas, Phys. Rev. **123,** 1242 (1961).

[40] J. H. Wilson, Y. Fu, S. Das Sarma, and J. H. Pixley, Disorder in twisted bilayer graphene, Phys. Rev. Res. **2,** 023325 (2020).

[41] N. Nakatsuji and M. Koshino, Moiré disorder effect in twisted bilayer graphene, Phys. Rev. B **105,** 245408 (2022).

[42] C. W. J. Beenakker, Guiding-center-drift resonance in a periodically modulated two-dimensional electron gas, Phys. Rev. Lett. **62,** 2020 (1989).

[43] A. Ya. Maltsev and S. P. Novikov, Open level lines of a superposition of periodic potentials on a plane, Ann. Phys. (Amsterdam) **447,** 169039 (2022).

[44] A. Rauh, G. H. Wannier, and G. Obermair, Bloch electrons in irrational magnetic fields, Phys. Status Solidi B **63,** 215 (1974).

[45] J. Avron and B. Simon, Singular continuous spectrum for a class of almost periodic Jacobi matrices, Bull. Am. Math. Soc. **6,** 81 (1982).

[46] M. Modugno, Exponential localization in one-dimensional quasi-periodic optical lattices, New J. Phys. **11,** 033023 (2009).

[47] F. H. Claro and G. H. Wannier, Magnetic subband structure of electrons in hexagonal lattices, Phys. Rev. B **19,** 6068 (1979).

[48] M. Wilkinson, Critical properties of electron eigenstates in incommensurate systems, Proc. R. Soc. A **391,** 305 (1984).

[49] M. Wilkinson, An exact renormalisation group for bloch electrons in a magnetic field, J. Phys. A **20,** 4337 (1987).

[50] J. H. Han, D. J. Thouless, H. Hiramoto, and M. Kohmoto, Critical and bicritical properties of harper's equation with next-nearest-neighbor coupling, Phys. Rev. B **50,** 11365 (1994).

[51] L. Yeo and P. J. Crowley, Non-power-law universal scaling in incommensurate systems, arXiv:2206.02810.

[52] It is straightforward to verify this argument for the square lattice potential whose extended levels sets run in the x (y) direction for $\lambda > 1$ ($\lambda < 1$).

[53] S. N. Shevchenko, S. Ashhab, and F. Nori, Landau–Zener–Stückelberg interferometry, Phys. Rep. **492,** 1 (2010).

[54] Y.-Z. Chou, F. Wu, and S. Das Sarma, Hofstadter butterfly and floquet topological insulators in minimally twisted bilayer graphene, Phys. Rev. Res. **2,** 033271 (2020).

[55] W. G. Chambers, Linear-network model for magnetic breakdown in two dimensions, Phys. Rev. **140,** A135 (1965).

[56] R. G. Chambers, Magnetic breakdown in real metals, Proc. Phys. Soc. London **88,** 701 (1966).

[57] V. A. Zakharov, A. M. Bozkurt, A. R. Akhmerov, and D. O. Oriekhov, Landau quantization near generalized Van Hove singularities: Magnetic breakdown and orbit networks, Phys. Rev. B **109,** L081103 (2024).

[58] G. Szego, *Orthogonal Polynomials*, 4th ed., Amer. Math. Soc. Colloq. Publ. Vol. 23 (American Mathematical Society, Providence, 1975).

[59] J. Finney, A. L. Sharpe, E. J. Fox, C. L. Hsueh, D. E. Parker, M. Yankowitz, S. Chen, K. Watanabe, T. Taniguchi, C. R. Dean, A. Vishwanath, M. A. Kastner, and D. Goldhaber-Gordon, Unusual magnetotransport in twisted bilayer graphene, Proc. Natl. Acad. Sci. U.S.A. **119,** e2118482119 (2022).

[60] A. Barelli, J. Bellissard, and F. Claro, Magnetic-field-induced directional localization in a 2D rectangular lattice, Phys. Rev. Lett. **83,** 5082 (1999).